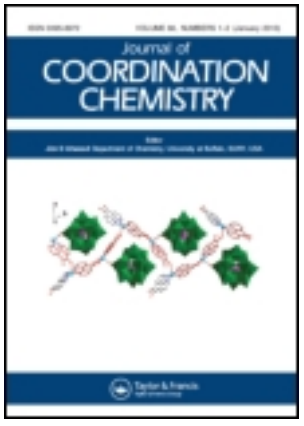

Journal of Coordination Chemistry
Publication details, including instructions for authors and subscription information:
http://www.tandfonline.com/loi/gcoo20

Hydrogen-bonded assemblies of a new polyoxometalate-based 3-D supramolecular architecture

Zhihui Yi [a], Xiao Zhang [a], Xiaoyang Yu [b], Lei Liu [a], Xianzhu Xu [a], Xiaobing Cui [c] & Jiqing Xu [c]

[a] State Key Laboratory of Urban Water Resource and Environment (SKLUWRE) & Academy of Fundamental and Interdisciplinary Sciences, Harbin Institute of Technology , Harbin, China

[b] Jilin Institute of Chemical Technology , Jilin City , China

[c] College of Chemistry and State Key Laboratory of Inorganic Synthesis and Preparative Chemistry, Jilin University , Jilin , China

Accepted author version posted online: 09 Apr 2013.Published online: 07 May 2013.

To cite this article: Zhihui Yi , Xiao Zhang , Xiaoyang Yu , Lei Liu , Xianzhu Xu , Xiaobing Cui & Jiqing Xu (2013) Hydrogen-bonded assemblies of a new polyoxometalate-based 3-D supramolecular architecture, Journal of Coordination Chemistry, 66:11, 1876-1888, DOI: 10.1080/00958972.2013.793795

To link to this article: http://dx.doi.org/10.1080/00958972.2013.793795

Journal of Coordination Chemistry, 2013
Vol. 66, No. 11, 1876–1888, http://dx.doi.org/10.1080/00958972.2013.793795

Hydrogen-bonded assemblies of a new polyoxometalate-based 3-D supramolecular architecture

ZHIHUI YI† and XIAO ZHANG*†, XIAOYANG YU‡, LEI LIU†, XIANZHU XU†, XIAOBING CUI§ and JIQING XU§

†State Key Laboratory of Urban Water Resource and Environment (SKLUWRE) & Academy of Fundamental and Interdisciplinary Sciences, Harbin Institute of Technology, Harbin, China
‡Jilin Institute of Chemical Technology, Jilin City, China
§College of Chemistry and State Key Laboratory of Inorganic Synthesis and Preparative Chemistry, Jilin University, Jilin, China

(*Received 16 January 2013; in final form 8 February 2013*)

A new hydrogen-bonded 3-D supramolecular architecture $[Ni(2,2'\text{-bpy})_3]_{1.5}[AsW^{VI}_{10}W^{V}_{2}O_{40}Ni(2,2'\text{-bpy})_2(H_2O)]\cdot 0.5H_2O$ (2,2′-bpy = 2,2′-bipyridine) (**1**) has been hydrothermally synthesized and characterized by single-crystal X-ray diffraction analysis, PXRD, elemental analysis, XPS, and IR spectrum. Compound **1** exhibits photocatalytic activity for methylene blue degradation under visible-light irradiation and shows good stability toward visible-light photocatalysis. Luminescence of **1** is also reported.

Keywords: Crystal structure; Hydrogen-bonded; Supramolecular network; Photocatalytic activity; Fluorescence

1. Introduction

Supramolecular chemistry has been defined as the understanding of intermolecular interactions in the context of crystal packing and the utilization of such understanding in design of new solids with desired physical and chemical properties [1, 2]. Supramolecular cements like O–H···O, N–H···O, C–H···O, and O–H···N hydrogen bonding interactions play crucial roles in crystal engineering of supramolecular assemblies [3–6]. Bipyridine-type ligands were applied to crystal engineering in the construction of metal-organic framework structures and coordination polymers [7–9]. Judicious placement of the pyridine nitrogen allows for design of specific supramolecular architectures [10]. Introducing coordination flexibility into such ligand gives access to a wider variety of structures and reduced ability to control the ultimate crystal structure.

*Corresponding author. Email: zhangx@hit.edu.cn

Supramolecular assemblies based on polyoxometalates (POMs) have been investigated in catalysis, nonlinear optical materials, and medicine [11–13]. Keggin-type POM $[XM_{12}O_{40}]^{n-}$ [X = a main group (such as P^{V}, Si^{IV}, Al^{III}, etc.) or a transition metal ion (such as Fe^{III}, Co^{II}, Cu^{I}, *etc*.) and M = transition metal ion] has been reported [14]. The Keggin-type structure of α-$[PW_{12}O_{40}]^{3-}$ was reported by Berzelius 100 years ago [15], with the spherical surface giving opportunity for forming hydrogen bonding interactions with organic/inorganic moieties. Efforts have been focused on design and assembly of such supramolecular architectures. Now, 1-, 2-, and even 3-D supramolecular architectures have been synthesized [16–19]. Reported work mostly focused on the structure of POMs, though hydrogen bonds were mentioned. The function of hydrogen bonds, which play an important role in formation of the overall configuration, was neglected in most cases.

Herein, we report a new compound $[Ni(2,2'\text{-bpy})_3]_{1.5}[AsW^{VI}{}_{10}W^{V}{}_{2}O_{40}Ni(2,2'\text{-bpy})_2(H_2O)]\cdot 0.5H_2O$ (**1**), in which Keggin polyanions are inorganic building blocks for constructing supramolecular arrays with metal-organic units. Hydrogen bonding interactions lead to the final overall 3D supramolecular architecture. Photocatalytic activity of **1** for decomposition of methylene blue (**MB**) under visible-light irradiation has been investigated, in which **1** exhibits good stability as a photocatalyst.

2. Experimental

2.1. *Materials and physical measurements*

All reagents used were of analytical grade and obtained from commercial sources without purification. Elemental analysis (C, H, and N) was performed on a Perkin-Elmer 2400 CHN Elemental Analyzer. IR (KBr pellets) spectrum was recorded from 300 to 4000 cm^{-1} using a Perkin-Elmer Spectrum One spectrophotometer. Solid diffuse reflectance UV−vis spectra were recorded on a Perkin-Elmer Lambda 750 ultraviolet spectrophotometer, whereas UV−vis spectra for solution samples were obtained on a HITACHI U-3900 spectrophotometer. Powder X-ray diffraction analysis was performed on a Bruker D8 Advance powder diffractometer using Ni-filtered Cu Kα radiation at 40 kV and 30 mA, from 10° to 30° with a scan rate of 0.3°s^{-1}. XPS analysis was performed on a VG ESCALAB MK II spectrometer with a Mg–Kα (1253.6 eV) achromatic X-ray source. Thermogravimetric analysis was performed on a Perkin-Elmer TGA-7000 instrument with a heating rate of 20 °C min^{-1} in air. Emission/excitation spectra were recorded on a RF-540 fluorescence spectrophotometer. Photocatalytic experiments in aqueous solutions were carried out in a 500 mL water-cooled quartz cylindrical vessel. The reaction mixture was maintained at room temperature by a continuous flow of water through an external cooling coil. The visible-light source was a 500 W Xe lamp (main output >400 nm). To establish an adsorption/desorption equilibrium of **MB** on the sample surface, a suspension of powdered catalyst (15 mg) in fresh aqueous solution of **MB** (50 mL, 5.0 mg L^{-1}) was magnetically stirred in the dark for at least 30 min in the vessel before irradiation. At given irradiation time intervals (30 min), a series of aqueous solutions of a certain volume were collected and separated through centrifuge to remove suspended catalyst particles and then subjected to UV–vis spectroscopic measurement. The concentration of organic dye was estimated by the absorbance at 665 nm, which directly relates to the structure change of its chromophore.

2.2. *Synthesis of [Ni(2,2′-bpy)$_3$]$_{1.5}$[AsW$_{12}$O$_{40}$Ni(2,2′-bpy)$_2$(H$_2$O)]·0.5H$_2$O (1)*

A mixture of $Na_3AsO_4 \cdot 12H_2O$ (0.1 g, 0.24 mmol), WO_3 (0.1 g, 0.43 mmol), $NiCl_2 \cdot 6H_2O$ (0.15 g, 0.63 mmol), 2,2′-bpy (0.1 g, 0.64 mmol), and H_2O (15 mL) was continuously stirred for 2 h in air at room temperature, and the pH was adjusted to 6.0 with sodium hydroxide aqueous solution. The resulting solution was sealed in a 20-mL Teflon-lined stainless steel vessel and heated at 180 °C for 3 days under autogenous pressure. After slowly cooling to ambient temperature, black block crystals were obtained and washed with distilled water. The yield based on W is 35%. Anal. Calcd. for $C_{65}H_{55}N_{13}O_{41.5}AsW_{12}Ni_{2.5}$ (%): C, 18.98; H, 1.34; N, 4.43. Found: C, 18.96; H, 1.25; N, 4.40.

2.3. *X-ray single-crystal structure determinations*

Compound **1** was studied on a Rigaku RAXIS–RAPID image plate area detector using graphite monochromated Mo Kα diffraction ($\lambda = 0.71073$ Å) at room temperature. A single crystal with dimensions $0.21 \times 0.15 \times 0.10$ mm was selected from the batch sample and mounted on a glass fiber. Data collection was in the range $3.03 \leqslant 2\theta \leqslant 27.48°$ with $-60 \leqslant h \leqslant +60$, $-18 \leqslant k \leqslant +18$ and $-33 \leqslant h \leqslant +33$. A total of 19,893 (1218 independent reflections, $R_{int} = 0.095$) reflections were measured. The maximum and minimum peaks on the final difference Fourier map corresponded to 3.566 and -3.326 eÅ^{-3}, respectively. The structure was solved by direct methods and refined by full-matrix least-squares based on F^2 using SHELXTL–97 crystallographic software package [20]. All nonhydrogen atoms were refined anisotropically. Positions of the hydrogens attached to carbons were fixed at their ideal positions and those attached to water oxygens were not located. The crystal parameters and experimental details of data collection are summarized in table 1.

Table 1. Crystal data and structure refinement for **1**.

Empirical formula	$C_{65}H_{55}N_{13}O_{41.5}AsW_{12}Ni_{2.5}$
Formula weight	4110.12
Crystal system	Monoclinic
Space group	*C2/c*
a/Å	46.738(9)
b/Å	14.313(3)
c/Å	26.011(5)
α/°	
β/°	90.14(3)
γ/°	
V/Å^3	17,400(6)
Z	8
D_c/Mg m^{-3}	3.138
μ/mm^{-1}	16.792
F (0 0 0)	14,872
R_{int} value	0.095
Goodness-of-fit on F^2	1.043
Final R^{ab} indices [$I > 2\sigma(I)$]	$R_1 = 0.0484$, $wR_2 = 0.1137$
R indices (all data)	$R_1 = 0.0813$, $wR_2 = 0.1261$

$^aR_1 = \Sigma||F_o| - |F_c||/\Sigma|F_o|$. $^bwR_2 = |\Sigma w(|F_o|^2 - |F_c|^2)^2/\Sigma|w(F_o^2)^2|^{1/2}$.

3. Results and discussion

3.1. *Crystal structure of 1*

The asymmetric unit of **1** consists of a α-Keggin polyanion $[AsW^{VI}_{10}W^{V}_{2}O_{40}]^{5-}$, a terminal unit $[Ni(2,2'\text{-bpy})_2(H_2O)]^{2+}$, one and a half free $[Ni(2,2'\text{-bpy})_3]^{2+}$, and half a free water (figure 1). As usually observed [21], the Keggin anion is composed of a central AsO_4 tetrahedron surrounded by 12 WO_6 octahedra with four W_3O_{13} linked by shared corners to each other and to the central tetrahedron. For AsO_4, the As–O distances are 1.651(7)–1.662(6) Å and O–As–O angles vary from 108.2(3) to 110.5(4)°. According to the different coordination environments in the polyanion, oxygens can be divided into four groups: O_t (terminal oxygen atoms connecting to one W) with W–O_t 1.672(9)–1.711(7) Å, O_b (the bridging O) with W–O_b 1.884(7)–1.963(7) Å, O_c (the O in the AsO_4 tetrahedron) with W–O_c 2.322(7)-2.379(7) Å, and O_a (connecting Ni and W, *i.e.*, O35) with W–O_a 1.711(7) Å, while bond angles at W range from 70.6(3) to 171.9(4)°. The $Ni(1)(2,2'\text{-bpy})_2(H_2O)$ is terminal, supported by each $[AsW^{VI}_{10}W^{V}_{2}O_{40}]^{5-}$ with Ni(1)–O(35) 2.079(7) Å, each Ni(1) completes octahedral configuration by a oxygen donor from a coordinated water and four nitrogen donors from two 2,2′-bpy, with Ni(1)–O(1 W) 2.102(9) Å and Ni(1)–N bond lengths ranging from 2.045(10) to 2.07(9) Å, respectively. For the charge-compensation $[Ni(2)(2,2'\text{-bpy})_3]^{2+}$ and $[Ni(3)(2,2'\text{-bpy})_3]^{2+}$ cations, the center Ni completes its octahedron by six nitrogens from three 2,2′-bpy with Ni–N 2.065(9)−2.105(12) Å for Ni(2) and 2.072(11)−2.109(9) Å for Ni(3), respectively. Selected bond lengths and angles are given in table 2.

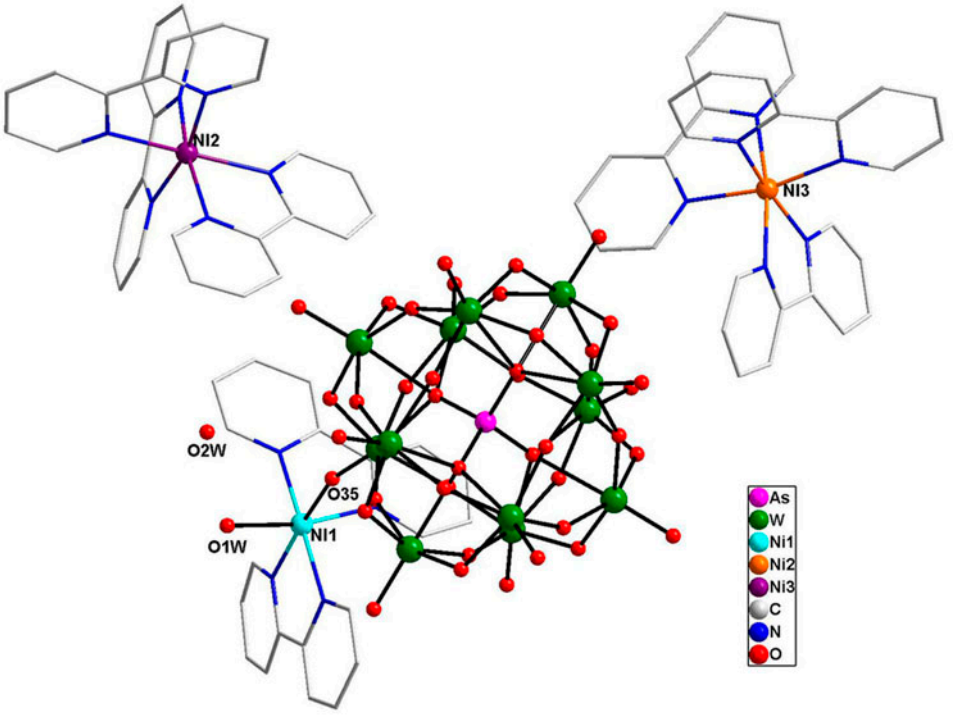

Figure 1. Perspective view of the crystal structure of **1**. All hydrogens are omitted for clarity.

Table 2. Selected bond lengths (Å) in **1**.

As(1)–O(12)	1.651(7)	W(8)–O(30)	1.688(7)
As(1)–O(13)	1.655(7)	W(8)–O(32)	1.904(7)
As(1)–O(20)	1.656(6)	W(8)–O(11)	1.924(8)
As(1)–O(24)	1.662(6)	W(8)–O(23)	1.938(7)
W(1)–O(38)	1.684(8)	W(8)–O(25)	1.939(7)
W(1)–O(23)	1.884(7)	W(8)–O(24)	2.363(7)
W(1)–O(10)	1.890(8)	W(9)–O(36)	1.691(8)
W(1)–O(16)	1.918(8)	W(9)–O(1)	1.884(8)
W(1)–O(4)	1.955(7)	W(9)–O(14)	1.900(7)
W(1)–O(20)	2.363(6)	W(9)–O(33)	1.914(8)
W(2)–O(31)	1.699(8)	W(9)–O(18)	1.938(7)
W(2)–O(2)	1.885(7)	W(9)–O(12)	2.322(7)
W(2)–O(25)	1.914(7)	W(10)–O(40)	1.682(8)
W(2)–O(3)	1.916(7)	W(10)–O(15)	1.890(7)
W(2)–O(17)	1.963(7)	W(10)–O(14)	1.906(8)
W(2)–O(24)	2.358(7)	W(10)–O(22)	1.912(8)
W(3)–O(19)	1.694(8)	W(10)–O(21)	1.959(8)
W(3)–O(5)	1.901(7)	W(10)–O(13)	2.345(7)
W(3)–O(6)	1.917(8)	W(11)–O(35)	1.711(7)
W(3)–O(16)	1.922(8)	W(11)–O(32)	1.898(8)
W(3)–O(2)	1.926(7)	W(11)–O(17)	1.921(8)
W(3)–O(20)	2.364(7)	W(11)–O(21)	1.921(8)
W(4)–O(34)	1.691(8)	W(11)–O(1)	1.926(8)
W(4)–O(26)	1.902(8)	W(11)–O(24)	2.316(6)
W(4)–O(8)	1.907(7)	W(12)–O(37)	1.672(9)
W(4)–O(29)	1.921(8)	W(12)–O(5)	1.891(7)
W(4)–O(33)	1.929(7)	W(12)–O(9)	1.914(8)
W(4)–O(12)	2.379(7)	W(12)–O(22)	1.915(7)
W(5)–O(39)	1.701(7)	W(12)–O(3)	1.937(7)
W(5)–O(4)	1.910(7)	W(12)–O(13)	2.336(7)
W(5)–O(8)	1.911(8)	Ni(1)–N(11)	2.045(10)
W(5)–O(7)	1.920(7)	Ni(1)–N(13)	2.064(10)
W(5)–O(6)	1.923(8)	Ni(1)–N(10)	2.070(9)
W(5)–O(20)	2.354(7)	Ni(1)–N(12)	2.070(11)
W(6)–O(27)	1.692(8)	Ni(1)–O(35)	2.079(7)
W(6)–O(29)	1.898(7)	Ni(1)–O(1W)	2.102(9)
W(6)-O(11)	1.902(8)	Ni(2)–N(1)	2.065(9)
W(6)–O(18)	1.912(7)	Ni(2)–N(2)	2.094(10)
W(6)–O(10)	1.920(7)	Ni(2)–N(3)	2.105(12)
W(6)–O(12)	2.362(7)	Ni(3)–N(8)	2.072(11)
W(7)–O(28)	1.685(8)	Ni(3)–N(7)	2.083(9)
W(7)–O(7)	1.899(7)	Ni(3)–N(5)	2.091(10)
W(7)–O(26)	1.916(8)	Ni(3)–N(6)	2.098(10)
W(7)–O(9)	1.923(8)	Ni(3)–N(9)	2.103(10)
W(7)–O(15)	1.931(7)	Ni(3)–N(4)	2.109(9)
W(7)–O(13)	2.359(7)		

Hydrogen bonds exist in **1**, making a robust 3-D supramolecular solid. Detailed analysis shows that intermolecular C–H···O and O–H···O hydrogen bonds coexist in **1**. As shown in figure 2(a), C(59) which belongs to $[AsW_{12}O_{40}Ni(1)(2,2'\text{-bpy})_2(H_2O)]^{3-}$ connects O(30) of the adjacent α-Keggin polyanion to build a 1-D supramolecular chain along the c axis with C(59)···O(30^{i}) 3.019(39) Å [symmetry code: (i) x, 1−y, 0.5+z]. For a $[Ni(2)(2,2'\text{-bpy})_3]^{2+}$, the central Ni(2) is at the special position (0, 0.182284, 0.25) and the site occupancy factor is 0.5. The C(31) and its symmetry related C(31^{iii}) [symmetry code: (iii) −z, y, 0.5−z] bridge two $[AsW_{12}O_{40}Ni(2,2'\text{-bpy})_2(H_2O)]^{3-}$ anion chains (as mentioned above) to form a 1-D double-chain structure perpendicular to the b axis with C(31)···O(37^{ii}) 3.086(36) Å [symmetry code: (ii) −x, −1+y, 0.5−z] [figure 2(b) left]. Figure 2(b)

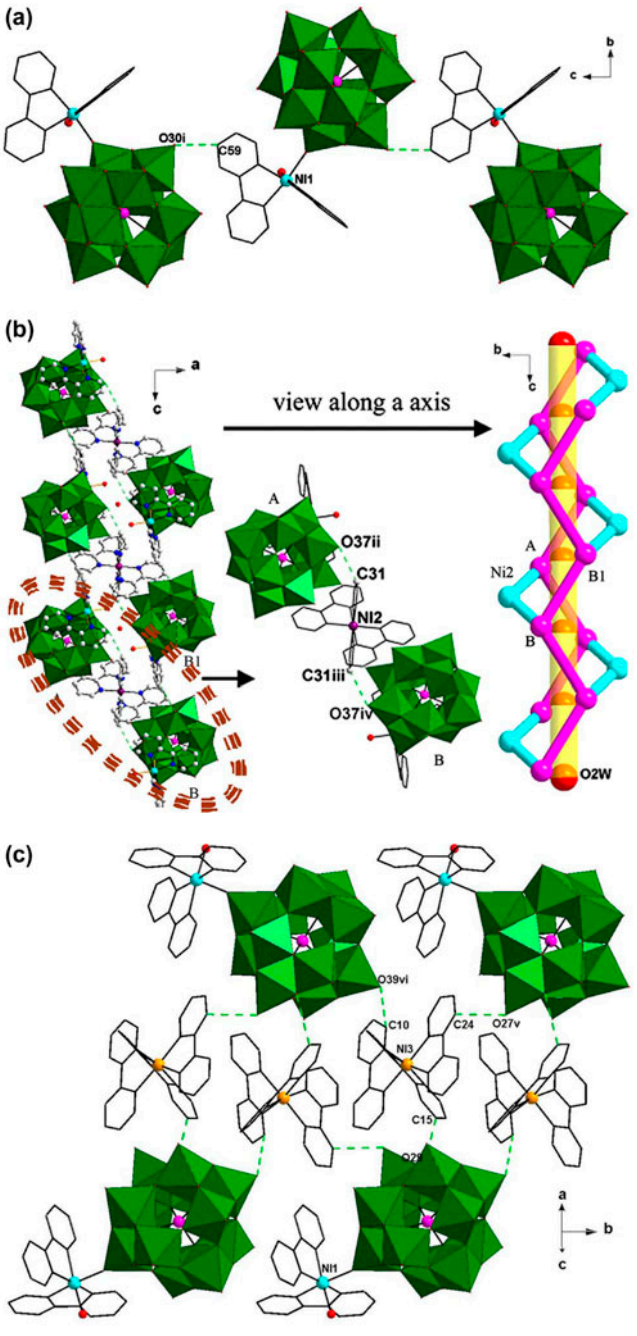

Figure 2. (a) Supramolecular interactions through $[AsW^{VI}_{10}W^{V}_{2}O_{40}Ni(2,2'\text{-bpy})_2(H_2O)]^{3-}$; (b) 1-D double-chain structure involving $[Ni(2)(2,2'\text{-bpy})_3]^{2+}$ interacting with polyanion and schematic illustrations (the right in which purple represents polyanions, the blue represent $[Ni(2)(2,2'\text{-bpy})_3]^{2+}$ and the red represent O(2 W); (c) the hydrogen bonds between polyanions and $[Ni(3)(2,2'\text{-bpy})_3]^{2+}$. All hydrogens are omitted for clarity. Symmetry codes: (i) x, 1−y, 0.5+z; (ii) −x, −1+y, 0.5−z; (iii) −z, y, 0.5−z; (iv) 0.5−x, −0.5+y, 0.5−z; (v) 0.5−x, 0.5+y, 0.5−z; (vi) 0.5−x, −0.5+y, 0.5−z.

(middle) clearly shows intermolecular C–H···O hydrogen bonds between two $[AsW_{12}O_{40}Ni(2,2'\text{-bpy})_2(H_2O)]^{3-}$ anions (A and B). The schematic illustration (right) reveals that the two supramolecular chains, which simultaneously display both beautiful sinusoid and cosine look, are further connected by $[Ni(2)(2,2'\text{-bpy})_3]^{2+}$ to form a pseudo-helix configuration with a 1-D channel. Interestingly, the O(2 W) at the special position (0, 0.5, 0.5) with site occupancy factor being 0.5 is the symmetry center of two Keggin (A and B1) anions. O(2 W) (red in the imagination column) fills in the center of the 1-D channel. The $[Ni(3)(2,2'\text{-bpy})_3]^{2+}$ cation offers three C donors [C(10), C(15), and C(24)], with C(24)···O(27^{v}) 2.919(1) Å, C(10)···O(39^{vi}) 2.968(3) Å, and C(15)···O(29) 3.074(43) Å, respectively [symmetry codes: (v) 0.5−x, 0.5+y, 0.5−z; (vi) 0.5–x, −0.5+y, 0.5−z], forming another 1-D double-chain structure along the *b* axis [figure 2(c)]. Thus, two 1-D double-chains based on Keggin–Ni(2) units and Keggin–Ni(3) units are vertical to each other and edge-sharing the $[AsW_{12}O_{40}Ni(2,2'\text{-bpy})_2(H_2O)]^{3-}$ anion along two directions to form the overall 3D supramolecular network (figure 3). Alternatively, each α-Keggin $[AsW_{12}O_{40}]^{5-}$ polyanion acts as a special hexadentate ligand coordinating to three cations through five C–H···O hydrogen bonds and one Ni(1)–O covalent bond; each $[AsW_{12}O_{40}Ni(2,2'\text{-bpy})_2(H_2O)]^{3-}$ connects five others to construct the overall 3D supramolecular network.

Besides intermolecular C–H···O hydrogen bonds, a dimer through O–H···O hydrogen bonds stabilizes the 3D framework in **1**. As shown in figure 3, coordinated O(1 W) links two adjacent polyanions by hydrogen bonds to construct a supramolecular dimer with O(1 W)···O(31^{vii}) 2.78(6) Å [symmetry code: (vii) −x, 1−y, 1−z] and O(1 W)···O(2 W)

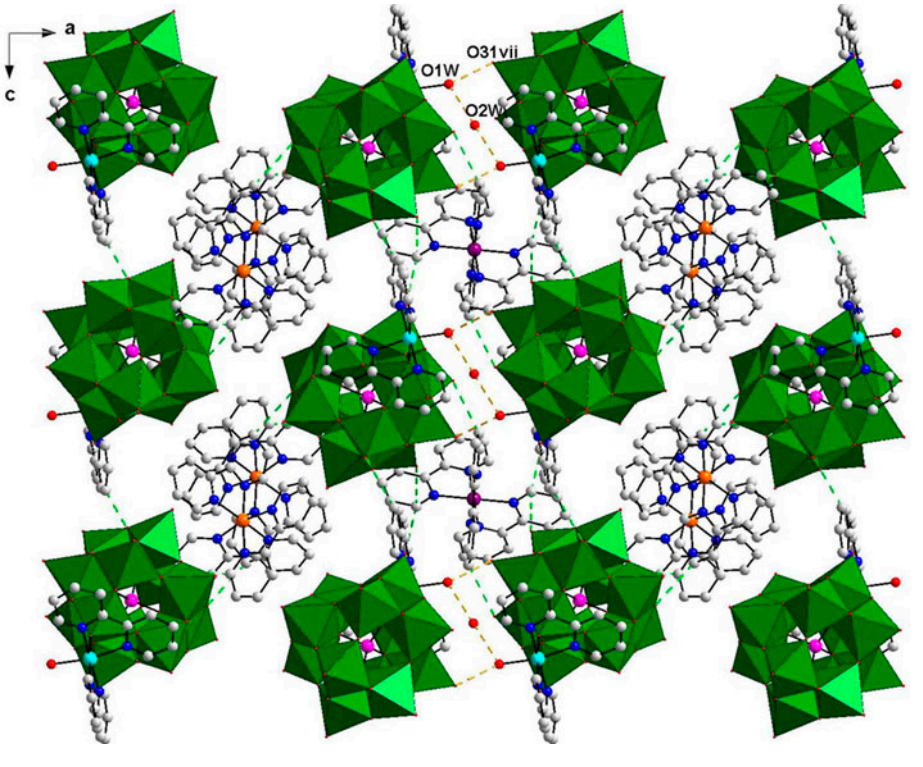

Figure 3. The 3D packing view and OW···O hydrogen bonds in **1**. Symmetry code: (vii) −x, 1−y, 1−z.

Table 3. Selected hydrogen bond lengths (Å) for **1**.

D···A	*d*(D–A)	D···A	*d*(D–A)
C(59)···O(30^{i})	3.019(39)	C(15)···O(29)	3.074(43)
C(31)···O(37^{ii})	3.086(36)	O(1 W)···O(31^{vii})	2.78(6)
C(24)···O(27^{v})	2.919(1)	O(1 W)···O(2 W)	2.956(6)
C(10)···O(39^{vi})	2.968(3)		

Symmetry codes: (i) x, 1−y, 0.5+z; (ii) −x, −1+y, 0.5−z; (iii) −z, y, 0.5−z; (v) 0.5−x, 0.5+y, 0.5−z; (vi) 0.5−x, −0.5+y, 0.5−z; (vii) −x, 1−y, 1−z.

Table 4. BVSs (Σ*s*) for **1**.

Atoms	Σ*s*	Atoms	Σ*s*
W1	6.27	W7	5.82
W2	5.73	W8	5.71
W3	5.77	W9	5.91
W4	5.80	W10	5.86
W5	5.75	W11	5.71
W6	5.89	W12	5.95

2.956(6) Å. The O(1 W)···O(31^{vii}) bond length is shorter than that of O(1 W)···O(2 W). From this, we speculate that formation of the dimer structure is probably that OW···O hydrogen bonds formed first and then stabilization by OW···OW hydrogen bonds. Selected hydrogen bonds are listed in table 3.

Bond valence sum (BVS) [22] calculation for **1** is listed in table 4. In **1**, the average value calculated for 10 W(VI) and 2 W(V) is 5.83, identical with the experimental value of 5.85. The BVS values of **1**, however, do not clearly identify the reduced W sites. This is due to delocalization of electrons on the reduced W centers over the polyanion framework involving all tungstens, as found in heteropolyblues [23]. In our experiments, some W(VI) were reduced to +5, suggesting that 2,2′-bpy is an effective agent for reducing W^{VI} to W^{V}. Organic amines such as 2,2′-bpy acting as reducing agents under hydrothermal conditions in the preparation of polyoxomolybdate have been reported [24].

3.2. *IR spectrum*

Bands from both organic and inorganic components of **1** were observed (suppilmentary material.docx). The strong bonds at 963, 791, and 732 cm^{-1} are assigned to the stretch of ν_{as}(W–O$_t$), ν_{as}(W–O$_b$), and ν_{as}(W–O$_c$) and 894 cm^{-1} is assigned to ν_{as}(As–O$_a$) bond, respectively. These bands can be easily assigned by comparing with the corresponding bands of Keggin polyanions [16, 18, 25]. Additional peaks of C–C, C=N, C–H, and C=C bonds occur at 2924, 1598, 1472, 1443, 1311, and 1154 cm^{-1}, confirming the presence of 2,2′-bpy in **1** [24]. The band at 3430 cm^{-1} in **1** suggests the presence of lattice water. The IR spectrum is in agreement with the result of X-ray diffraction structural analysis.

3.3. *XPS spectrum*

The XPS spectrum of **1** (figure 4) shows four overlapped peaks at 34.3, 35.3, 36.5, and 37.4 eV, ascribed to W^{5+} $4f_{7/2}$, W^{6+} $4f_{7/2}$, W^{5+} $4f_{5/2}$, and W^{6+} $4f_{5/2}$, respectively, further confirming the mixed valences of W in **1**.

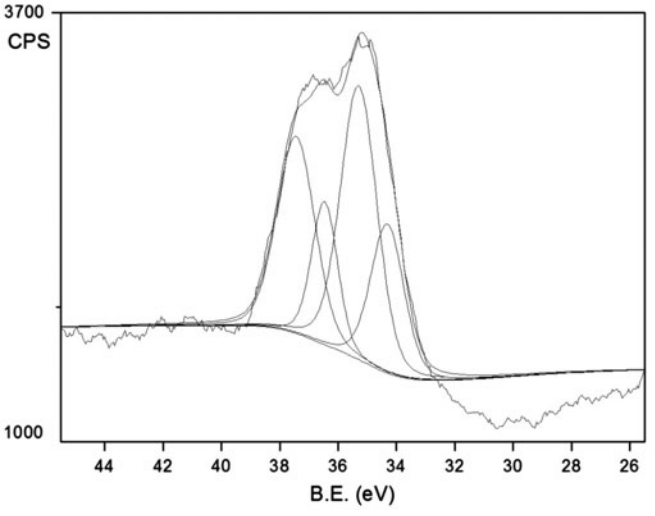

Figure 4. The XPS spectrum of W in **1**.

3.4. *Thermal analysis*

The TG curve of **1** continues its weight loss from 100 to 700 °C (Supplementary material); the whole loss (27.84%) is consistent with the calculated value (27.77%).

3.5. *Luminescence*

The solid luminescence at room temperature of **1** and free 2,2′-bpy has been investigated (figure 5). Comparing with the emission peak at 383 nm ($\lambda_{ex} = 256$ nm) of free 2,2′-bpy, the similar emission at 385 nm with the photoexcitation wavelength at 260 nm of **1** may be assigned to the π^*-π transitions of 2,2′-bpy.

3.6. *Optical energy gap*

Narrow gap semiconductor photocatalysts present excellent photocatalytic activities for degradation of organic pollutants in water utilizing energy from sunlight. Several POM-based inorganic–organic compounds have been reported as promising semiconductors, such as $[Cu(HL)_2(Mo_8O_{26})]\cdot H_2O$ ($E_g = 1.72$ eV) [26a], $[Cu_8$(1,3-bis(1,2,4-triazol-1-yl) propane)$_8[Mo_{12}O_{46}(AsPh)_4]_2]\cdot H_2O$ ($E_g = 1.72$ eV) [26b], and $Co_2(bpy)_6(W_6O_{19})_2$ ($E_g = 2.2$ eV) [26c]. In order to explore the conductivity of **1**, the measurement of diffuse reflectivity for powder sample was used to achieve its band gap (photoresponse wavelength region, E_g), which is determined as the intersection point between the energy axis and the line extrapolated from the linear portion of the adsorption edge in a plot of the Kubelka-Munk function F against E_g [26].

As shown in figure 6, the corresponding well-defined optical absorption associated with E_g can be assessed at 2.5 eV for **1**. The reflectance spectrum measurement reveals the presence of an optical band gap and the nature of semiconductivity of **1**, which indicates that **1** possesses possible potential for visible-light photocatalytic activity.

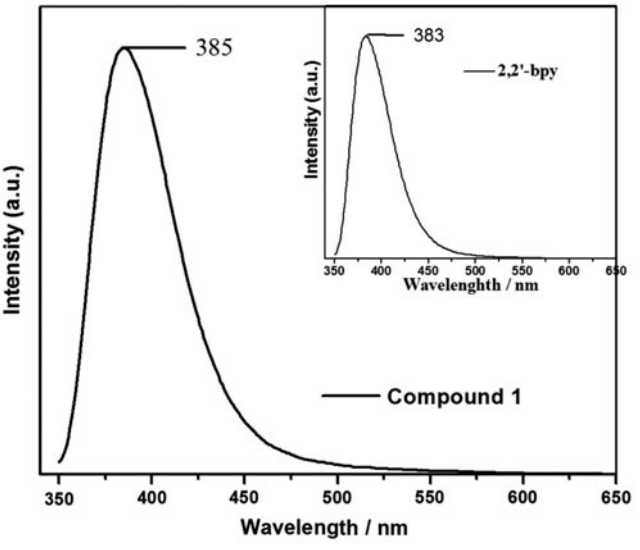

Figure 5. Luminescence spectra of **1** and 2,2′-bpy in the solid state at room temperature.

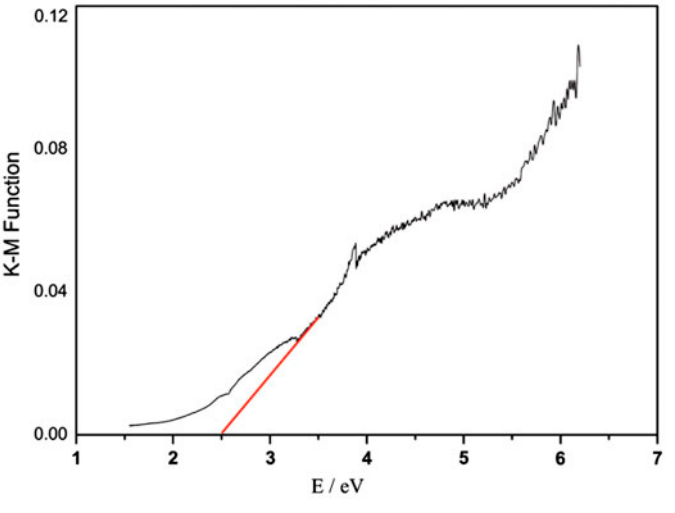

Figure 6. Kubelka-Munk-transformed diffuse reflectance spectrum of **1**.

3.7. *Photocatalysis property*

Photocatalytic properties of POMs have attracted attention because of their applications in purifying air and water [27]. During the process of photocatalytic degradation of organic dyes with POM catalysts, the organic materials were oxidized and chromophores were decomposed to nonpolluting small molecules. However, the synthesis and preparation of POMs with high photocatalytic activity is challenging [28]. Herein, **1** was tested for photocatalytic degradation of **MB**. A suspension containing **1** (15 mg) and 50 mL **MB** ($5.0\,mg\,L^{-1}$) solution was stirred in the dark for over 30 min. It was then stirred

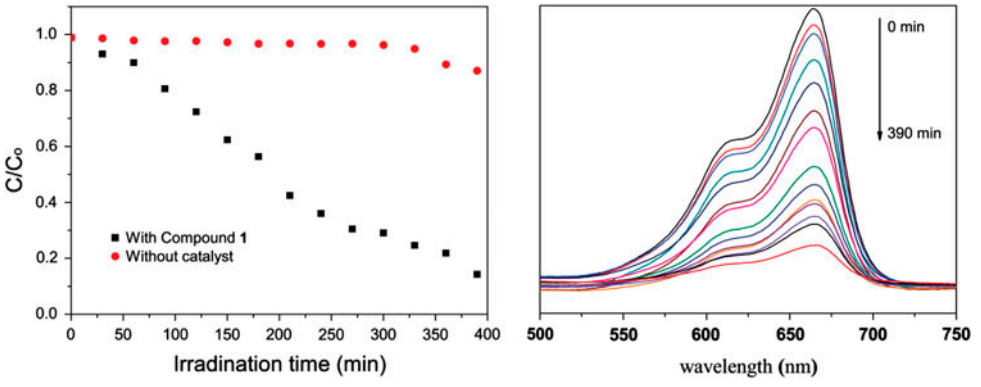

Figure 7. (A) Plots of concentration versus irradiation time for (red) **MB** under Xe lamp irradiation without photocatalyst, (black) **MB** under Xe lamp irradiation in the presence of **1**. (B) UV−vis absorption spectra of the **MB** solution during the decomposition reaction under visible-light irradiation in the presence of **1** (see http://dx.doi.org/10.1080/00206814.2013.793795 for color version).

continuously under xenon-lamp irradiation. Every 30 min, 3 mL of samples was taken out of the reactor for analysis. As illustrated in figure 7, the concentration of MB versus reaction time of **1** was plotted. It can be seen that photocatalytic activity increases from 13.1% (without any catalyst) to 85.7% (with **1**) after 390 min of irradiation. Although photocatalytic properties for POMs in aqueous solutions have been documented in the literature, the report about POMs modified by TMCs as photocatalysts is rare [26].

The color of **1** remains unchanged after photocatalysis. The photostability of **1** was monitored by using powder XRD patterns to check the structure during the course of photocatalytic reactions. A set of well-resolved sharp diffraction peaks featured for **1** before and after photocatalysis and the simulated pattern is shown in figure 8. The powder XRD pattern of **1** before and after a photocatalysis process is in agreement with the one

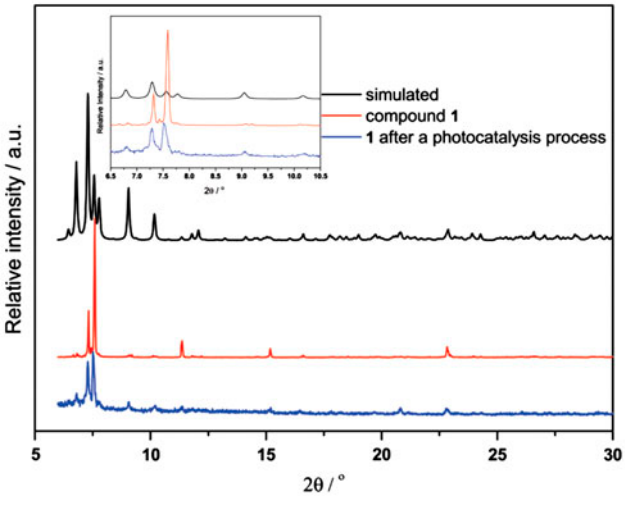

Figure 8. Powder XRD patterns of the simulated diagram from single-crystal data of **1** (black), **1** (red), **1** after a photocatalysis process (blue) (see http://dx.doi.org/10.1080/00206814.2013.793795 for color version).

simulated based on single-crystal structure data, which not only indicates that **1** is pure and could be used for investigation of photocatalysis, but also implies that **1** maintains its structural integrity after photocatalysis reaction, confirming that its stability toward photocatalysis is good.

4. Conclusion

In this paper, a new supramolecular assembly of Keggin heteropolyanions supporting transition metal complexes has been successfully synthesized. The detailed formation process of the supramolecular network was performed and analyzed with proof of bond lengths and bond angles. Supramolecular interactions among the organic molecules and inorganic polyanions play significant roles in stabilization of the overall 3-D supramolecular network. This work shows that such large assembly may be designed and synthesized according to the inherent stereo and interactive information stored in the organic molecules and inorganic anions. In addition, the 3-D supramolecular **1** shows photocatalytic activity under visible-light irradiation.

Supplementary material

CCDC 637069 contains the supplementary crystallographic data for **1**. The data can be obtained free of charge via http://www.ccdc.cam.ac.uk/conts/retrieving.html, or from the Cambridge Crystallographic Data Center, 12 Union Road, Cambridge CB2 1EZ, UK; Fax: (+44) 1223-336-033; or E-mail: deposit@ccdc.cam.ac.uk.

Acknowledgements

The work is supported by the National Natural Science Foundation (No. 51108122), Open Project of State Key Laboratory of Urban Water Resource and Environment, Harbin Institute of Technology (No. QA201025), The Fundamental Research Funds for the Central Universities (Grant No. HIT. NSRIF. 2010053) and Science and Technology Innovation Talents Special Foundation of Harbin (2010RFQXG035 and 2007RFXXG018).

References

[1] (a) J.M. Lehn. *Angew. Chem., Int. Ed. Engl.*, **29**, 1304 (1990); (b) J.M. Lehn, *Supramolecular Chemistry*, VCH: Weinheim (1995); (c) C.N.R. Rao, S. Natarajan, R. Vaidhyanathan. *Angew. Chem., Int. Ed.*, **43**, 1466 (2004); (d) S. Roy, K. Biradha. *Cryst. Growth Des.*, **9**, 4120 (2011).
[2] O.M. Yaghi, M. O'Keeffe, N.W. Ockwig, H.K. Chae, M. Eddaoudi, J. Kim. *Nature*, **423**, 705 (2003).
[3] E. Coronado, J.R. Galán-Mascarós, C. Giménez-Saiz, C.J. Gómez-García, S. Triki. *J. Am. Chem. Soc.*, **120**, 4671 (1998).
[4] B.J. Holliday, C.A. Mirkin. *Angew. Chem. Int. Ed.*, **40**, 2022 (2001).
[5] (a) D.K. Kumar, A. Das, P. Dastidar. *CrystEngComm*, **8**, 805 (2006); (b) C.S. Lai, F. Mohrb, E.R.T. Tiekink. *CrystEngComm*, **8**, 909 (2006); (c) I. Goldberg, S. Muniappan, S. George, S. Lipstman. *CrystEngComm*, **8**, 784 (2006).
[6] (a) W. Kan, J. Yang, Y. Liu, J. Ma. *Polyhedron*, **30**, 2106 (2011); (b) C. Wang, C. Yang, W. Chung, G. Lee, M. Ho, Y. Yu, M. Chung, H. Sheu, C. Shih, K. Cheng, P. Chang, P. Chou. *Chem. Eur. J.*, **17**, 9232 (2011).

[7] A.J. Blake, N.R. Champness, P. Hubberstey, W.S. Li, M.A. Withersby, M. Schröder. *Coord. Chem. Rev.*, **183**, 117 (1999).
[8] P.J. Hagrman, D. Hagrman, J. Zubieta. *Angew. Chem. Int. Ed.*, **38**, 2638 (1999).
[9] M.J. Zaworotko. *Chem. Commun.*, **1**, (2001).
[10] A.Y. Robin, K.M. Fromm. *Coord. Chem. Rev.*, **250**, 2127 (2006).
[11] L. Xiao, Y. Wang, Y. Peng, G. Li, J. Xu, L. Wang, Y. Hu, T. Wang, Z. Gao, D. Zheng, X. Cui. *J. Inorg. Chim. Acta*, **387**, 204 (2012).
[12] D. Li, P. Yin, T. Liu. *Dalton Trans.*, 2853 (2012).
[13] Z. Fu, Y. Zeng, X. Liu, D. Song, S. Liao, J. Dai. *Chem. Commun.*, **48**, 6154 (2012).
[14] M.T. Pope. *Heteropoly and Isopoly Oxometalates*. p. 26, Springer-Verlag, Berlin (1983).
[15] J.F. Keggin. *Nature*, **131**, 908 (1933).
[16] (a) X.C. Huang, J.P. Zhang, Y.Y. Lin, X.L. Yu, X.M. Chen. *Chem. Commun.*, 1100 (2004); (b) J.P. Zhang, S.L. Zheng, X.C. Huang, X.M. Chen. *Angew. Chem., Int. Ed.*, **43**, 206 (2004); (c) M. Wei, H. Li, G. He. *J. Coord. Chem.*, **64**, 4318 (2011); (d) J. Ying, M. Hou, X.J. Liu, A.-X. Tian, X.-L. Wang. *J. Coord. Chem.*, **65**, 218 (2012); (e) J. Wu, C. Wang, K. Yu, Z. Su, Y. Yu, Y. Xu, B. Zhou. *J. Coord. Chem.*, **65**, 69 (2012).
[17] (a) H.G. Harvey, B. Slater, M.P. Attfield. *Chem. Eur. J.*, **10**, 3270 (2004); (b) X.H. Bu, M.L. Tong, H.C. Chang, S. Kitagawa, S.R. Batten. *Angew. Chem., Int. Ed.*, **43**, 192 (2004); (c) C.M. Liu, S. Gao, D.Q. Zhang, Y.H. Huang, R.G. Xiong, Z.L. Liu, F.C. Jiang, D.B. Zhu. *Angew. Chem., Int. Ed.*, **43**, 990 (2004); (d) B. Zhao, P. Cheng, X.Y. Chen, C. Cheng, W. Shi, D.Z. Liao, S.P. Yan, Z.H. Jiang. *J. Am. Chem. Soc.*, **126**, 3012 (2004).
[18] (a) T. Akutagawa, F. Kudo, R. Tsunashima, S. Noro, L. Cronin, T. Nakamura. *Inorg. Chem.*, **50**, 6711 (2011); (b) T. Noguchi, C. Chikara, K. Kuroiwa, K. Kanekob, N. Kimizuka. *Chem. Commun.*, **47**, 6455 (2011); (c) P. Shringarpure, B.K. Tripuramallu, K. Patel, A. Patel. *J. Coord. Chem.*, **64**, 4016 (2011); (d) A.-X. Tian, X.-L. Lin, Y.-J. Liu, G.-Y. Liu, J. Ying, X.-L. Wang, H.-Y. Lin. *J. Coord. Chem.*, **65**, 2147 (2012).
[19] (a) Z. Yi, X. Yu, W. Xia, L. Zhao, C. Yang, Q. Chen, X. Wang, X. Xu, X. Zhang. *CrystEngComm*, **12**, 242 (2010); (b) C. Liu, D.-Q. Zhang, D.-B. Zhu. *Cryst. Growth Des.*, **5**, 1639 (2005); (c) T. Arumuganathan, A. S. Rao, S.K. Das. *Cryst. Growth Des.*, **10**, 4272 (2010); (d) X. Wang, Y. Guo, Y. Li, E. Wang, C. Hu, N. Hu. *Inorg. Chem.*, **42**, 4135 (2003); (e) Y.-W. Li, Y.-G. Li, Y.-H. Wang, X.-J. Feng, Y. Liu, E.-B. Wang. *Inorg. Chem.*, **48**, 6452 (2009); (f) R. Yang, S.-X. Liu, Q. Tang, S.-J. Li, D.-D. Liang. *J. Coord. Chem.*, **65**, 891 (2012).
[20] G.M. Sheldrick. *SHELXL 97, Program for Crystal Structures Refinement*, University of Göttingen, Germany (1997).
[21] Y. Xu, J.Q. Xu, K.L. Zhang, Y. Zhang, X.Z. You. *Chem. Commun.*, **153**, (2000).
[22] I.D. Brown. In *Structure and Bonding in Crystals*, M. O'Keeffe, A. Navrotsky (Eds.), Vol. II, p. 1, Academic Press, New York (1981).
[23] (a) M.T. Pope, A. Müller. *Angew. Chem., Int. Ed. Engl.*, **34**, 30 (1991); (b) G.M. Varga, J.E. Papaconstantinou, M.T. Pope. *Inorg. Chem.*, **9**, 662 (1970).
[24] F. Li, L. Xu, Y. Wei, Y. Qiu, Z. Wang, E. Wang. *J. Coord. Chem.*, **58**, 1751 (2005).
[25] J. Sha, Y. Zhang, S. Li, L. Liu, L. Liang, H. Yan, H. Zhang. *J. Mol. Struct.*, **975**, 211 (2010).
[26] (a) H.-Y. Zang, Y.-Q. Lan, G.-S. Yang, X.-L. Wang, K.-Z. Shao, G.-J. Xu, Z.-M. Su. *CrystEngComm*, **12**, 434 (2010); (b) B. Liu, Z.-T. Yu, J. Yang, W. Hua, Y.-Y. Liu, J.-F. Ma. *Inorg. Chem.*, **50**, 8967 (2011); (c) L. Zhang, Y. Wei, C. Wang, H. Guo, P. Wang. *J. Solid State Chem.*, **177**, 3433 (2004).
[27] (a) H. Lin, P. A. Maggard. *Inorg. Chem.*, **47**, 8044 (2008); (b) M.Y. Dong, Q. Lin, H.M. Su, D. Chen, T. Zhang, Q.Z. Wu, S.P. Li. *Cryst. Growth Des.*, **11**, 5002 (2011).
[28] (a) Y. Hu, F. Luo, F. Dong. *Chem. Commun.*, **47**, 761 (2011); (b) A. Mylonas, A. Hiskia, E. Papaconstantinou. *J. Mol. Catal. A: Chem.*, **114**, 191 (1996); (c) A. Mylonas, E. Papaconstantinou. *J. Photochem. Photobiol. A*, **94**, 77 (1996).